JOURNAL OF GEOPHYSICAL RESEARCH, VOL. 90, NO. B6, PAGES 4511-4528, MAY 10, 1985

MICROEARTHQUAKE SEISMICITY AND FAULT PLANE SOLUTIONS RELATED TO ARC-CONTINENT COLLISION IN THE EASTERN SUNDA ARC, INDONESIA

Robert McCaffrey, Peter Molnar, and Steven W. Roecker

Department of Earth, Atmospheric, and Planetary Sciences, Massachusetts Institute of Technology, Cambridge

Yoko S. Joyodiwiryo[1]

Geological Research and Development Centre, Bandung, Indonesia

Abstract. The collision of Australia with the eastern Sunda and Banda arcs of Indonesia represents a modern example of the early stages of arc-continent collision. In order to obtain a more detailed view of the tectonics of the collision zone, a microearthquake survey was conducted around the Savu Sea, the region that encompasses the transition from subduction of Indian Ocean lithosphere on the west to collision or subduction of Australian continental lithosphere on the east. Intermediate depth earthquakes were concentrated near Pantar Island, the easternmost active volcano of the Sunda arc, and outline a northwest dipping zone that strikes N65°E from 70 to 150 km depth. The seismic zone probably marks the western edge of the collision zone and its more northerly strike, and the orientations of nodal planes from fault plane solutions indicate a 25° bend in the subducted slab to a depth of at least 150 km. Because the convergence rate and the timing of collision from geologic observations on Timor suggest that the part of the slab now at 150 km depth was at the trench when Australia first collided with Timor, we infer that continental crust (or at least rifted continental margin crust) caused the bend in the convergent margin and has been subducted to 150 km depth. Fault plane solutions of several events show nearly vertical nodal planes that trend parallel to the strike of the seismic zone, along which a northwest-side-down sense of displacement is indicated: these events are concentrated at the southern (top) side of the seismic zone and suggest that the subducted lithosphere is presently detaching in the 50-100 km depth range beneath the eastern Savu Sea. Fault plane solutions for earthquakes within the upper part of the detaching slab (70-100 km depth) have P and T axes whose trends lie parallel to the strike of the seismic zone and horizontal, southeast trending B axes. These earthquakes are interpreted as due to stresses caused by the bend in the subducting plate.

Introduction

Our understanding of the response of continental lithosphere to the subduction process is limited by the difficulty of identifying such interactions in the geologic record and the paucity of sites at which continental subduction is presently occurring. It is commonly believed that the buoyancy of continental crust would prevent it from being subducted [McKenzie, 1969], but no unequivocal evidence has been presented to disprove that some length could be pulled into the asthenosphere by the leading, subducting oceanic plate [Molnar and Gray, 1979]. The longevity of continental masses compared to oceanic lithosphere alone tells us that continents are more resistant to the subduction process. Geologic structures suggest that collisions of continents with other continents or island arcs may result in continental accretion and the development of mountain belts rather than in destruction of continental crust.

The ongoing collision of the eastern Sunda and Banda arcs of eastern Indonesia with the Australian continental shelf offers an excellent modern setting to study the processes of continental subduction and collision. Subduction of both the Australian continental shelf and slope and of the Indian Ocean lithosphere as parts of a single plate beneath the Java trench and Timor trough forms a long and continuous island arc system on the southern perimeter of the Indonesian archipelago. The contrast in average density between Australian continental lithosphere and oceanic lithosphere beneath the Indian Ocean could lead to large stresses near the boundary between them as they subduct. If subduction of the continental lithosphere is inhibited, the oceanic lithosphere may detach from the continental part, and this process should be evident in lateral variations in structure along the convergent margin.

In this paper we present the results of a microearthquake survey conducted in 1982 in the region of the Australia-Sunda arc convergence zone where the Australian continental slope enters the Timor trough. The distribution of accurately located microearthquakes and their fault plane solutions have allowed a more detailed view than has previously been possible of the geometry of and the state of stress within the slab subducted beneath Timor. These observations are valuable in understanding the mechanics of arc-continent collision and the history of convergence in the Timor area.

Tectonic Setting

The Indian Ocean-Australian plate is moving northward relative to southeast Asia and subducts beneath the southern Indonesian islands along the Java trench and Timor trough (Figure 1). From

[1]Now at the Marine Geological Institute of the Geological Survey of Indonesia, Bandung, Indonesia

Paper number 4B5177.
0148-0227/85/004B-5177$05.00

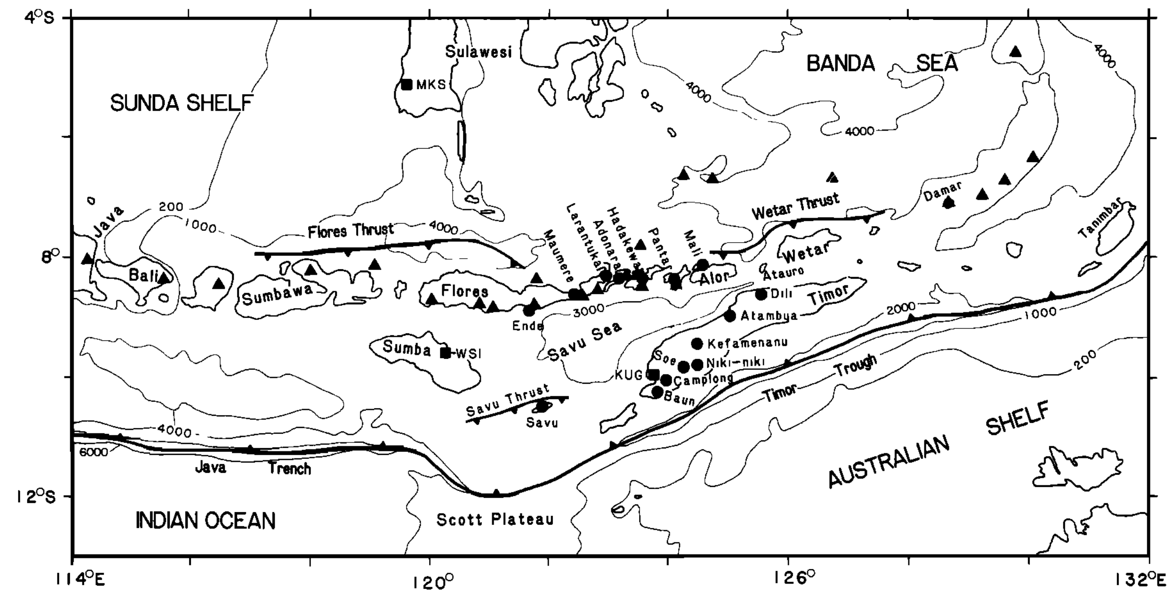

Fig. 1. Tectonic map of the eastern Sunda and Banda arcs, eastern Indonesia. Dots and squares show positions of temporary and permanent seismograph stations, respectively. Solid triangles represent active volcanoes. Bathymetric contours are marked in meters.

Java to near Sumba (119°E), the Indian Ocean lithosphere bends down to form the deep Java trench and plunges northward into the asthenosphere to depths in excess of 600 km (Figure 2) [Cardwell and Isacks, 1978]. East of 123°E the floor of the trench is much shallower than to the west, and continental crust of the Australian shelf is found on the seaward side. Seismic refraction profiles shot in the Timor trough (about 9°S, 129°E) reveal depths to the Moho of 27 km [Curray et al., 1977] and 30-40 km [Jacobson et al., 1979], indicative of continental crust.

The islands from Java to Pantar (Figure 1) are part of the long, active volcanic arc that forms the southern perimeter of Indonesia. Between Pantar and Damar, the line of active volcanoes is interrupted for a stretch of 600 km, but it continues east of Damar. Parallel to and south of the volcanic chain, a nonvolcanic outer arc includes the islands of Sumba, Savu, Timor, and Tanimbar (Figure 1). The latter three of these islands are extensively deformed and indicate a long history of convergence along the Timor trough. In contrast, the island of Sumba is relatively undeformed and is most likely an

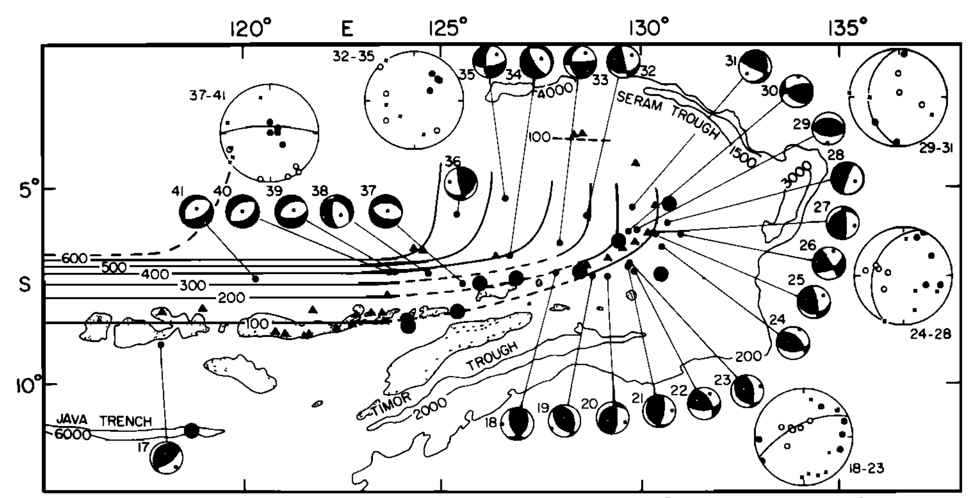

Fig. 2. Fault plane solutions for deep and intermediate depth earthquakes along the eastern Sunda and Banda arcs [from Cardwell and Isacks, 1978]. Shaded quadrants show compressional first motions. Contours to the top of the seismic zone are shown by heavy lines, dashed where uncertain, and are marked in kilometers. The large circles are lower hemisphere plots of the P (dots), T (circles), and B (crosses) axes for the numbered solutions, and lines through the solutions show the local orientation of the seismic zone. Triangles show the positions of active volcanoes, and large circles mark large shallow earthquakes (M ≥ 7) since 1900.

TABLE 1. Data for Temporary Seismograph Stations

Station Site	Latitude °S	Longitude °E	Elevation, m	Operation Dates	Clock σ, s
Lamahala, Adonara	8.392	123.157	10	Aug. 14 - Sept. 16	0.50
Atambua, Timor	9.092	123.888	350	June 30 - Sept. 15	0.08
Baun, Timor	10.308	123.667	400	July 21 - Aug. 23	0.15
Camplong, Timor	10.050	123.917	700	July 22 - Aug. 22	0.08
Dili, Timor	8.582	125.575	100	Sept. 2 - Sept. 16	1.00
Ende, Flores	8.818	121.645	200	June 30 - Sept. 15	0.03
Hadakewa, Lembata	8.383	123.537	40	July 2 - Sept. 16	0.10
Kefamenanu, Timor	9.442	124.475	540	June 27 - Sept. 15	0.06
Larantuka, Flores	8.270	122.992	20	June 29 - Aug. 3	1.00
Larantuka (II)	8.338	122.980	50	Aug. 4 - Sept. 16	0.15
Mali, Alor	8.143	124.582	50	July 11 - Sept. 16	0.10
Maumere, Flores	8.632	122.220	55	June 25 - Aug. 3	0.06
Maumere (II)	8.648	122.198	50	Aug. 5 - Sept. 16	0.06
Niki-niki, Timor	9.808	124.467	780	July 28 - Aug. 12	0.08
Puntaro, Pantar	8.463	124.073	100	July 8 - July 17	0.05
Baranusa, Pantar	8.395	124.082	200	July 18 - Sept. 16	0.05
Savu	10.485	121.870	50	June 30 - Sept. 16	0.25
Soe, Timor	9.907	124.307	815	June 30 - Sept. 16	0.07

uplifted portion of the forearc underlain by continental or unusually thick oceanic crust [Chamalaun et al., 1982].

Several observations taken together imply that subduction of some continental lithosphere has occurred along the eastern Sunda arc. The deep bathymetric expression of the Java trench abruptly ends where the Australian shelf intersects it between 122° and 123°E (Figure 1). Bathymetric profiles across the Timor trough, however, show an amount of deflection of the Australian continental plate similar to that of its oceanic counterpart at the Java trench to the west. Seismic reflection and refraction profiles reveal continuity of continental crust from Australia to the Timor trough [Beck and Lehner, 1974; Bowin et al., 1980; Curray et al., 1977; Jacobson et al., 1979; von der Borch, 1979], and gravity anomalies suggest that the crust continues to thicken beneath Timor [Chamalaun et al., 1976]. The high concentrations of strontium and lead isotopes in late Cenozoic and Recent lavas from volcanoes along the eastern Sunda arc east of 120°E suggest contamination by continentally derived sediments [Whitford et al., 1977; Whitford and Jezek, 1979] or continental crust [Morris, 1983]. These various observations require that the Australian shelf has underthrust Timor and are consistent with as much as 200 km of subduction of continental crust.

Studies of the geology of Timor have led to conflicting interpretations, but most workers agree that Permian to Jurassic sedimentary rocks that were formerly part of the Australian continental margin underlie most of the island. A major controversy is centered on the identification of a series of thrust sheets of Permian to Pliocene rocks that now overlie the Australian facies rocks. Audley-Charles et al. [1974] and Carter et al. [1976] suggest that the thrust sheets have little resemblance to those of similar age on the Australian margin and that the rocks in them are of Asian origin. This interpretation places the initial contact point between Asia and Australia in central Timor. If, as is undoubtedly the case [Fitch and Hamilton, 1974], the Timor trough is the present site of subduction, this scenario suggests that the deformed rocks of southern Timor (along with their continental basement) have been accreted to the Asian plate and that thrusting subsequently shifted southward to the Timor trough. Alternatively, others [Chamalaun; 1977a,b; Fitch and Hamilton, 1974; Grady, 1975; Hamilton, 1977] suggest that there are in fact similarities among the postulated thrust sheets, the underlying pre-Cretaceous rocks, and present day Australian continental margin rocks. The latter interpretation implies that southern Timor represents an uplifted accretionary prism and is consistent with the Timor trough being the site of past and present subduction.

There are indications, however, that not all of the relative convergence between Australia and Eurasia from Java to Timor (calculated to be approximately 75 km/m.y. [Minster and Jordan, 1978]) is taken up presently at the Timor trough. The paucity of shallow seismicity (Hamilton [1974], Cardwell and Isacks [1978] and this study) and an absence of large, underthrusting earthquakes beneath the forearc region near Timor suggest that little, or modified, motion occurs between the plates. On the basis of their calculation of sedimentation rates by correlating age dates from Deep Sea Drilling Project hole 262 with sediment thicknesses from seismic reflection profiles, Johnston and Bowin [1981] suggest that points now on the seaward slope of the Timor trough have had fairly constant sedimentation rates over the past half million years. They interpret this as meaning that these points have not moved toward the higher sedimentation rates that they infer occur deeper in the trough and therefore that only a few kilometers of convergence have occurred at the Timor trough during this time. Bowin et al. [1980] suggest that convergence in the Timor region is accommodated instead by deformation distributed throughout the forearc. This view is supported by the more northeasterly trend of the Timor trough than that of the Java trench, suggesting that the trench south of Timor has migrated to the north relative

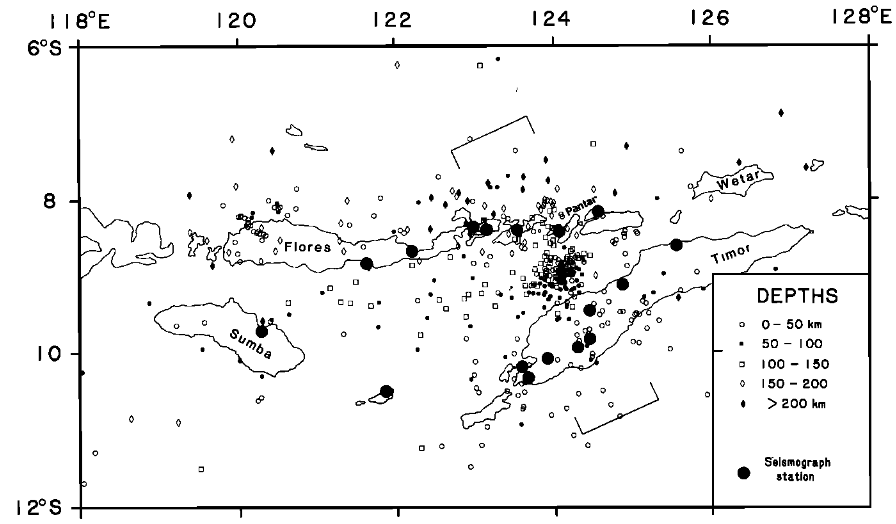

Fig. 3. Map of earthquake epicenters located by the local array. The brackets show the projection area of Figure 9. Events of all quality classifications are shown.

to the Banda Sea. The deflection of the volcanic arc north of Timor, however, indicates that at least some of the convergence occurs in the back arc region.

In the back arc, a long fault zone accommodates underthrusting of the back arc basin crust southward beneath the arc [Hamilton, 1979; Silver et al., 1983; Usna et al., 1979]. The thrust is well developed north of Sumbawa, Flores, Alor, and Wetar but is absent or obscured between central Flores and western Alor [Silver et al., 1983]. The thrust zone is associated with large gravity anomalies and large thrust earthquakes [McCaffrey and Nabelek, 1984a, b].

Studies of the seismicity of the eastern Sunda arc have revealed continuity at depths greater than 300 km beneath the Sunda and Banda arcs [Hatherton and Dickinson, 1969; Fitch and Molnar, 1970; Fitch 1970, 1972; Hamilton, 1974; Cardwell and Isacks, 1978]. West of 124°E the intermediate depth (i.e., 70-300 km depth) seismic zone is fairly well defined, but earthquakes at these depths are absent from 124°E to 127°E, where the volcanic arc is quiescent [Cardwell and Isacks, 1978]. Fault plane solutions for shallow earthquakes have been determined by Fitch [1972], Cardwell and Isacks [1978], Kappel [1980], and McCaffrey and Nabelek [1984a, b] and indicate thrust faulting beneath Sumba and the back arc region, strike slip beneath the arc and forearc, and normal faulting beneath the Java trench. No solutions have been found for shallow earthquakes beneath the forearc near Timor.

An analysis of the 100-km-deep earthquake beneath the Banda Sea in 1963 led Osada and Abe [1981] to postulate a break within the subducted slab at about 130°E. On the basis of relocations of teleseismically recorded earthquakes and their fault plane solutions, McCaffrey [1981] suggested that a tear separates the continental from oceanic lithosphere within the subducting slab north of Timor (at 124°E). Tearing of the Indian Ocean plate at the Java trench may also have caused the great 1977 Sumba earthquake [Given and Kanamori, 1980]. The results presented here strongly support these interpretations.

Data

The data we present and use are the locations of approximately 460 microearthquakes and 45 fault plane solutions obtained by an array of portable seismograph stations that operated for 10 weeks on the islands surrounding the Savu Sea (Table 1 and Figure 1). In addition, the fault plane solutions and depths of two large events from 1970 and 1978 were obtained from the analysis of long-period P and SH waveforms. The details of the survey and data analysis are left to the appendix and will be summarized briefly here. Other results and logistical details of the survey are presented by McCaffrey et al. [1984].

The microearthquakes (Figure 3) were located assuming the velocity structure in Table 2 and calculated locations were classified as A, B, or

TABLE 2. Velocity Models

Earthquake Location

Depth to Top of Layer, km	V_p, km/s
0	6.00
15	6.75
25	8.00
85	8.10
150	8.20
200	8.30
250	8.50
300	8.70
400	9.10

Waveform Synthesis

Depth to top of Layer, km	V_p, km/s	V_s, km/s	Density, kg/m^3
0	1.5	0.0	1.0
3	6.2	3.6	2.8
28	8.1	4.6	3.3

TABLE 3. Fault Plane Solutions From Microearthquakes

						Plane 1		Plane 2		P axis		T axis	
No.	Date 1982	Time	Latitude °S	Longitude °E	Depth km	Az, deg	Dip, deg	Az, deg	Dip, deg	Az, deg	Pl, deg	Az, deg	Pl, deg
1	July 5	0034	9.316	121.314	127	250	60	70	30	160	75	340	15
2	July 16	1005	8.927	123.904	106	275	55	95	35	185	80	5	10
3[a]	July 16	1250	9.412	122.636	119	135	90	45	35	15	35	255	35
4	July 16	2146	9.233	123.653	102	200	65	20	25	110	70	290	20
5[a,b]	July 16	2236	7.665	124.654	359	30	60	130	73	353	34	258	8
6[a]	July 17	0916	8.901	124.062	109	240	50	90	44	85	74	344	3
7	July 18	2046	9.688	124.466	49	160	40	70	90	127	33	13	33
8[a]	July 20	0629	9.240	122.433	83	70	90	250	0	160	45	340	45
9	July 25	1125	9.231	122.920	113	210	45	69	52	141	4	41	69
10	July 26	0846	8.436	123.430	197	160	75	285	25	234	27	96	55
11[a]	July 30	1231	8.923	124.229	75	165	70	44	36	277	19	37	55
12	Aug. 1	1632	8.967	124.102	81	130	50	352	48	241	1	333	68
13[a]	Aug. 2	1049	9.057	124.034	46	85	3	265	87	175	48	355	42
14[a]	Aug. 3	2102	9.228	123.691	85	50	60	230	30	140	15	320	75
15[c]	Aug. 6	2040	8.102	120.522	25	50	85	141	80	5	11	96	4
16[c]	Aug. 6	2046	8.180	120.643	26	30	80	122	80	346	14	76	0
17[a]	Aug. 7	0600	9.082	123.817	79	170	80	350	10	260	35	80	55
18[a]	Aug. 7	0615	9.231	123.742	75	190	30	22	61	108	16	307	74
19	Aug. 7	1154	10.001	124.494	42	140	45	270	57	125	62	23	7
20[a]	Aug. 7	1229	8.886	124.181	81	15	60	195	30	105	15	285	75
21	Aug. 8	0658	8.941	124.049	97	170	35	350	55	80	10	260	80
22	Aug. 9	0315	9.742	121.341	2	130	37	310	53	220	82	40	8
23	Aug. 9	1052	8.055	124.001	185	20	70	290	90	243	14	337	14
24[a]	Aug. 9	2143	8.882	124.094	104	350	70	247	57	213	39	116	8
25[a]	Aug. 10	1956	9.021	122.965	54	140	25	288	69	177	64	28	23
26[a]	Aug. 10	2148	8.897	124.218	88	15	80	195	10	105	35	285	55
27[a]	Aug. 11	1028	8.939	124.100	86	85	85	201	11	166	39	6	49
28[a]	Aug. 12	2139	8.063	124.003	190	150	85	59	75	15	14	284	7
29	Aug. 15	0714	8.590	122.794	191	110	60	290	30	20	75	200	15
30	Aug. 16	1904	8.956	124.121	90	120	35	300	55	210	80	30	10
31	Aug. 18	1322	8.713	124.475	129	15	80	195	10	105	35	285	55
32[a]	Aug. 20	1822	8.727	124.181	116	130	85	310	0	220	43	40	47
33	Aug. 23	0938	8.679	124.398	116	50	90	230	0	140	45	320	45
34[a]	Aug. 24	2036	9.018	124.032	99	145	80	325	10	235	35	55	55
35	Aug. 27	1723	8.829	122.211	102	170	35	20	59	329	71	98	12
36	Aug. 27	2143	8.810	123.953	111	110	80	290	10	200	35	20	55
37	Aug. 28	1609	9.911	124.430	50	350	65	211	32	226	64	95	17
38[a]	Sept. 2	1830	8.664	123.093	183	130	75	310	15	220	30	40	60
39	Sept. 3	1529	8.961	124.074	92	165	75	345	15	75	60	255	30
40[a]	Sept. 4	2111	8.586	124.005	132	220	70	26	21	138	65	306	25
41[a]	Sept. 10	0732	9.113	123.880	96	240	85	143	35	118	40	358	31
42	Sept. 10	1235	9.486	125.049	4	200	70	20	20	290	25	110	65
43	Sept. 10	1723	8.023	124.009	191	205	65	48	27	95	68	303	19
44[a]	Sept. 12	0606	8.677	123.926	118	100	60	231	41	59	62	169	10
45	Composite					165	35	310	60	178	68	54	13

[a] Better quality solutions.
[b] Based on first motion polarities taken from the Earthquake Data Report
[c] Based on waveform modeling from McCaffrey and Nabelek [1984b].

C in order of decreasing reliability. The criteria for rating the reliability are based on a series of tests and some statistical results of the location procedure, all described in the appendix. We tested for the effects on the locations of variations in the subset of stations recording the individual events, uncertainty in the estimate of the ratio of P to S wave velocities, and uncertainty in the knowledge of crustal and upper mantle velocity structure.

The tests indicate that location accuracy depends most heavily on the number of P and S phases used in the calculation and the position of the event relative to the network. Depth accuracy is critically dependent on the distance to the closest stations and on the availability of S phases. The locations of class A events probably have relative uncertainties of 5 km in depth and epicenter when they occur south of Pantar Island (Figure 3) and of twice this value throughout the rest of the network. B events have uncertainties of twice the A events for a given location with respect to the network. The epicentral uncertainties associated with C events are probably similar to those of B events when inside the array, but depth calculations are usually unreliable for C-type earthquakes.

The earthquake locations were plotted in maps,

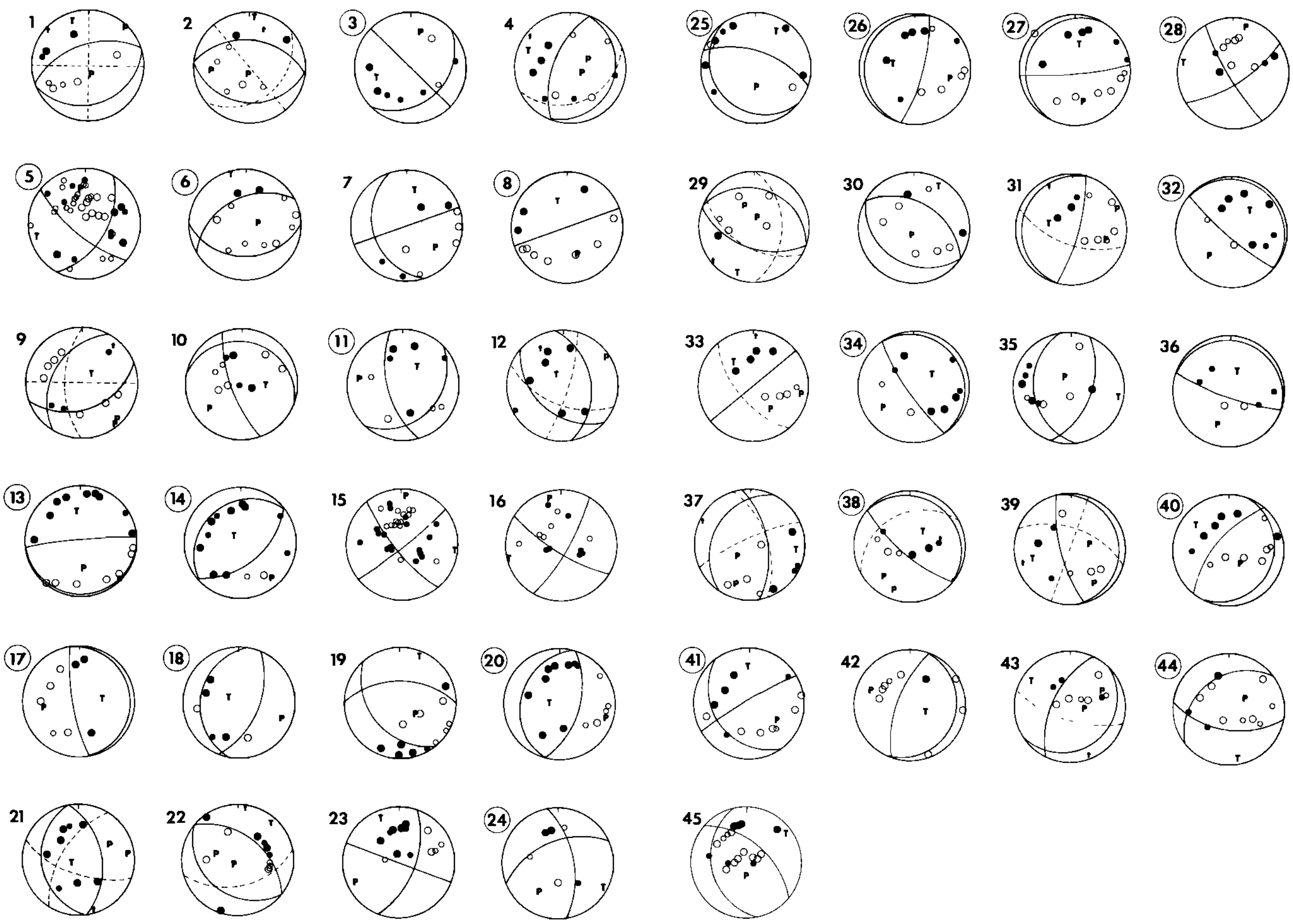

Fig. 4. Lower hemisphere projections of first motions and fault plane solutions determined in this study. Solid dots represent compressional first motions, and open circles are dilatations. Large and small symbols represent "strong" and "weak" first motions, respectively. Dashed lines show alternative nodal planes, and their P and T axes are shown by the lowercase letters. Solution parameters are listed in Table 3, and those with circled numbers designate better quality solutions. Solutions 15 and 16 were obtained from waveform modeling [McCaffrey and Nabelek, 1984b], rather than from the first motion data shown.

cross sections at varying azimuths, and in stereo pairs to determine the three-dimensional distribution of seismicity. Here, we have chosen to show events of all classes A, B, and C in the plots to avoid biasing the view by selectively deleting events that may have C classifications because of their location with respect to the network. For example, there is a preference for the shallowest events to have a C classification because of the requirement for A and B events that a station be within two focal depths. Excluding C-type events would thus remove most of the shallow earthquakes and lead to the erroneous conclusion that there is little shallow seismicity. In later figures the different class events are plotted with different size dots, with class A events being the largest.

Individual fault plane solutions for 44 microearthquakes and a composite solution for one group of events were obtained using the polarities of P waves at local stations (Table 3 and Figure 4). Takeoff angles were determined using the P wave velocities in Table 2; the uncertainties for upgoing rays due to uncertainties in the structure and focal depths are only a few degrees. Solutions and the P, T, and B axes were graded according to the extent to which they are constrained by the first motion data. In the figures and tables, reliable fault plane solutions (with uncertainties in orientations of about 30° or less) are distinguished from the poorer ones, and only the well-constrained P and T axes are presented.

The largest earthquakes to have occurred within the seismic zone south of Pantar in recent years are those of June 28, 1970, and February 12, 1978. We inverted long-period P and SH waveforms for source time function, orientation of the double couple, and source depths of these two events (Figure 5 and Table 4). The velocity structure used to generate the synthetic seismograms (Table 2) represents an average of that used to locate the microearthquakes, but it contains fewer layers to simplify the calculation of response functions. The 1970 and 1978 earthquakes were also relocated relative to the largest event recorded by the temporary network (event 13 in Table 3) and are presented here at

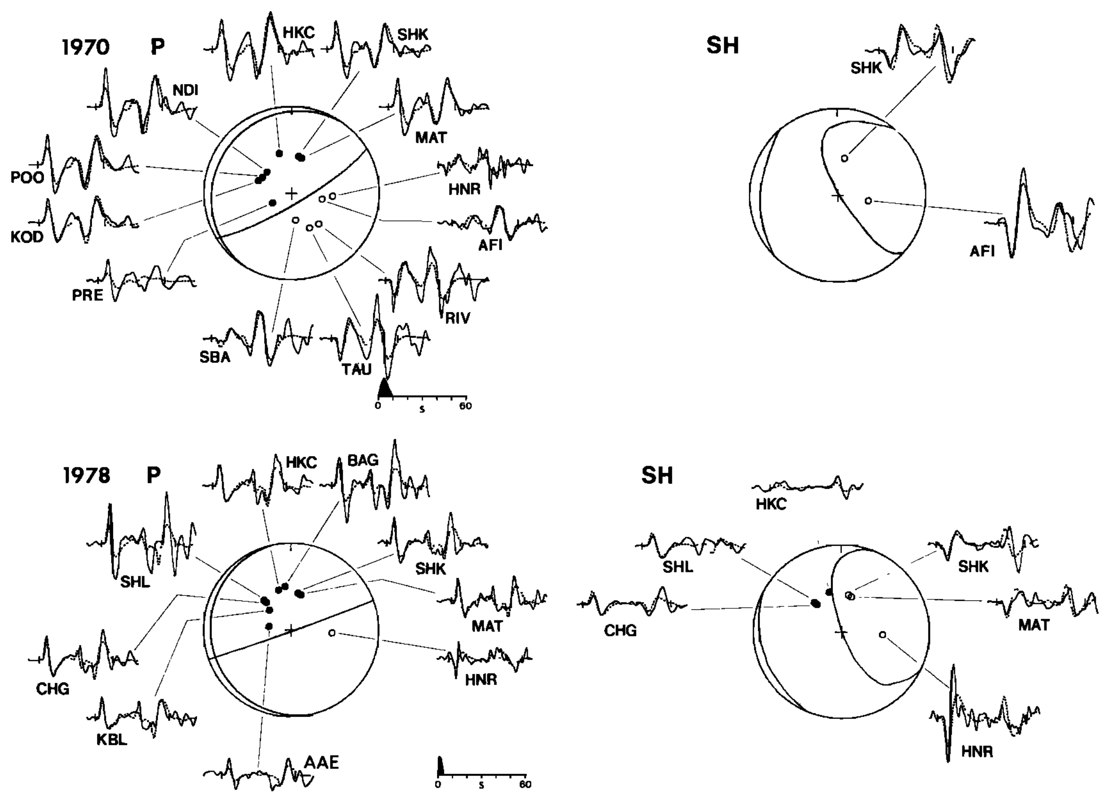

Fig. 5. Fault plane solutions for the earthquakes of 1970 and 1978 based on inversion of long-period P and SH waveforms. Details of the solutions are given in Table 4, and the assumed source structure is given in Table 2. Observed waveforms are shown by solid lines and computed waveforms by dotted lines. The tic marks on the seismograms enclose the data used in the inversion. The source time functions are shown on the time scale axes. Synthetic seismograms are scaled to the seismic moment, and both the observed and synthetic seismograms are scaled to a common distance and instrument magnification. Amplitudes of the SH waves are scaled down by a factor of 2 relative to the P waves.

the relocated positions. Again, the reader is directed to the appendix for additional information on procedures.

Results

A notable concentration of recorded events lies north of western Timor (8°S, 124°E) in the depth range of 70-200 km (Figures 3 and 6). A second pocket of seismicity occurred at shallow depth near 8°S, 120°E but is mainly associated with two large events that occurred there on August 6. Otherwise, seismicity is scattered beneath both the central Savu Sea and the island of Timor.

In Figure 7a the locations for 8 events are compared with the locations reported in Preliminary Determination of Epicenters (PDE) by the U.S. Geological Survey [1982]. There are no apparent correlations between differences in locations and numbers of stations or region. All differences in epicenters are less than 30 km, but depths could differ by as much as 50 km, with a tendency for PDE depths to be greater. Also shown are the resulting shifts in the epicenters of the 1970 and 1978 earthquakes when they are relocated relative to event 13 (Figure 7b).

In Figure 8 all hypocenters are projected onto an east-west striking vertical plane roughly parallel to the eastern Sunda arc and the Java trench. Seismicity to a depth of 200 km is fairly uniform between 120°E and 123°E. The apparent quiescence below 200 km is probably due to the poor resolution of locations of earthquakes occurring both to the north of the array and at depths larger than the dimensions of the array.

The large concentration of activity beneath 124°E between 70 and 200 km depth is due in part to the sensitivity of the array for events in this area, but it is also reflected in the distribution of larger earthquakes recorded teleseismically [Cardwell and Isacks, 1978; McCaffrey, 1981]. Therefore it is not an artifact of the short recording period. Equally as striking is the pronounced quiescence in seismic activity east of 124.5°E and most of this seismic activity is shallow. Deeper, there are only two well-located (class B) events, and both are deeper than 300 km. The quiescence at intermediate depths east of 124.5°E is also reflected in longer-term seismicity patterns [Fitch, 1970; Fitch and Molnar, 1970; Cardwell and Isacks, 1978].

The class A hypocenters from north of western Timor form the narrowest zone when projected onto a vertical plane at an azimuth of N25°W, indica-

TABLE 4. Fault Plane Solutions for Earthquakes of 1970 and 1978

	Date	
	June 28, 1970	Feb. 12, 1978
Origin time	0130:25.6	0334:38.3
Latitude	8.98°S	8.82°S
Longitude	124.12°E	124.04°E
Depth	80 km	107 km
Seismic Moment (dyn cm)	117×10^{24}	6×10^{24}
Plane 1		
Az	59°	70°
Dip	80°	89°
Plane 2		
Az	212°	166°
Dip	11°	9°
P axis		
Az	145°	151°
Pl	35°	43°
T axis		
Az	335°	349°
Pl	55°	45°

ting that the seismic zone strikes approximately N65°E in the 70-150 km depth range (Figure 9). Note that the 100-km contour (separating open squares and solid circles in Figure 3) is aligned approximately parallel to N65°E and not to the overall trend of the arc or to local trends of epicenters in this depth range west of this area (Figure 6). The N65°E trend, however, lies parallel to the Timor trough and the structural grain of Timor itself, suggesting that the surfacial bend in the arc is accompanied by a similar northward bend in the subducted plate to at least 150 km depth and possibly deeper.

Although the nodal planes from fault plane solutions (Figure 10) show a variety of orientations in the small area near Pantar, there is a general tendency for reverse faulting at depths shallower than 100 km and for normal faulting below 100 km. At depths less than 100 km in the region south of Pantar (Figure 10, top right), fault plane solutions can be divided into two groups: those that have nodal planes that trend parallel to the seismic zone and those that have nodal planes striking north or northwest, roughly perpendicular to the seismic zone. Events in the first group (A) have similar P, T, and B axes and are due to either dip-slip faulting along vertical to steeply south dipping planes (southside up) or underthrusting along shallow north dipping planes. These solutions show T axes roughly aligned with the plunge of the seismic zone.

The second group (B in Figure 10) is characterized by gently dipping to horizontal B axes that trend southeasterly and P and T axes that form a trend roughly parallel to the strike of the seismic zone but at variable plunges. These solutions indicate compressional and extensional trends in a direction parallel to the strike of the slab.

Fault plane solutions for events between 100 and 130 km depths in the Pantar region (Figure 10, group C) show some grouping of the P axes but with considerable scatter in the T axes. The B axes tend to be aligned roughly parallel to the seismic zone. Farther north and deeper (Figure 10, bottom left), solution 28 at 190 km depth and solution 5 at 359 km depth reveal gently north dipping P axes and nearly horizontal T axes.

An interesting feature of the seismic zone is the suggestion of two zones separated by an aseismic region between depths of 100 and 200 km directly below the volcanic arc (Figure 9). The earthquakes in the upper zone are well located, and their separation from the other group is real. However, we cannot be convinced that the aseismic gap between the two groups is not an artifact of the short recording period. The apparent double seismic zone here is not an artifact of the projection, as the separate zones are at approximately the same longitude but at different latitudes; the upper zone is visible in map view in the 100-150 km depth range plot in Figure 6 as a second NE trending zone just south of 8°S, 124°E.

Solution 45 (Figures 4 and 11) is a composite fault plane solution obtained from several small events that form the upper zone of the double seismic zone. This solution is not significantly different from those of the C group of fault plane solutions in the lower zone (Figure 10). In contrast, earthquake mechanisms from Japan [Hasegawa et al., 1978] have shown that the two zones of the double seismic zone are under different orientations of stress; downdip P axes in the upper zone and downdip T in the lower one. The stress differences may be due to unbending of the lithosphere [Engdahl and Scholz, 1977]. The similarity of the stress axes in both zones beneath Pantar indicates that unbending is not an important source of stress in the slab here.

Earthquakes occurred in two depth groups beneath Timor: very shallow (≤15 km) and in the 40-60 km depth range (Figure 9). The depths of the shallower events are poorly constrained, but short intervals between S and P arrivals from other smaller earthquakes at stations on Timor require depths as shallow as 10 km or less [McCaffrey et al., 1984]. The events at 40-60 km depth appear to be part of the projection of the intermediate depth seismic zone from north of Timor toward the Timor trough. These earthquakes probably occur within the Australia-Indian Ocean plate subducted at the Timor trough. Nevertheless, a gap in seismicity between the events beneath Timor and the intermediate depth seismic zone beneath 9°S (Figure 9) keeps the inference of continuity unproven.

West of 123°E hypocenters outline a northerly dipping zone in which there is considerable scatter in the locations (Figure 12). Fairly well-defined easterly elongated envelopes around the epicenters in the depth ranges greater than 100 km can be seen in Figure 6, implying an easterly striking seismic zone consistent with the findings of Hamilton [1974] and Cardwell and Isacks [1978]. Therefore the scatter in Figure 12 is probably due to the poor resolution of focal depths for events beneath the Savu Sea and not due to an inappropriate projection.

Fault plane solutions for earthquakes beneath Timor and the Savu Sea (Figures 10 and 12) show predominantly dip-slip mechanisms, but orientations of the nodal planes vary greatly. Solutions

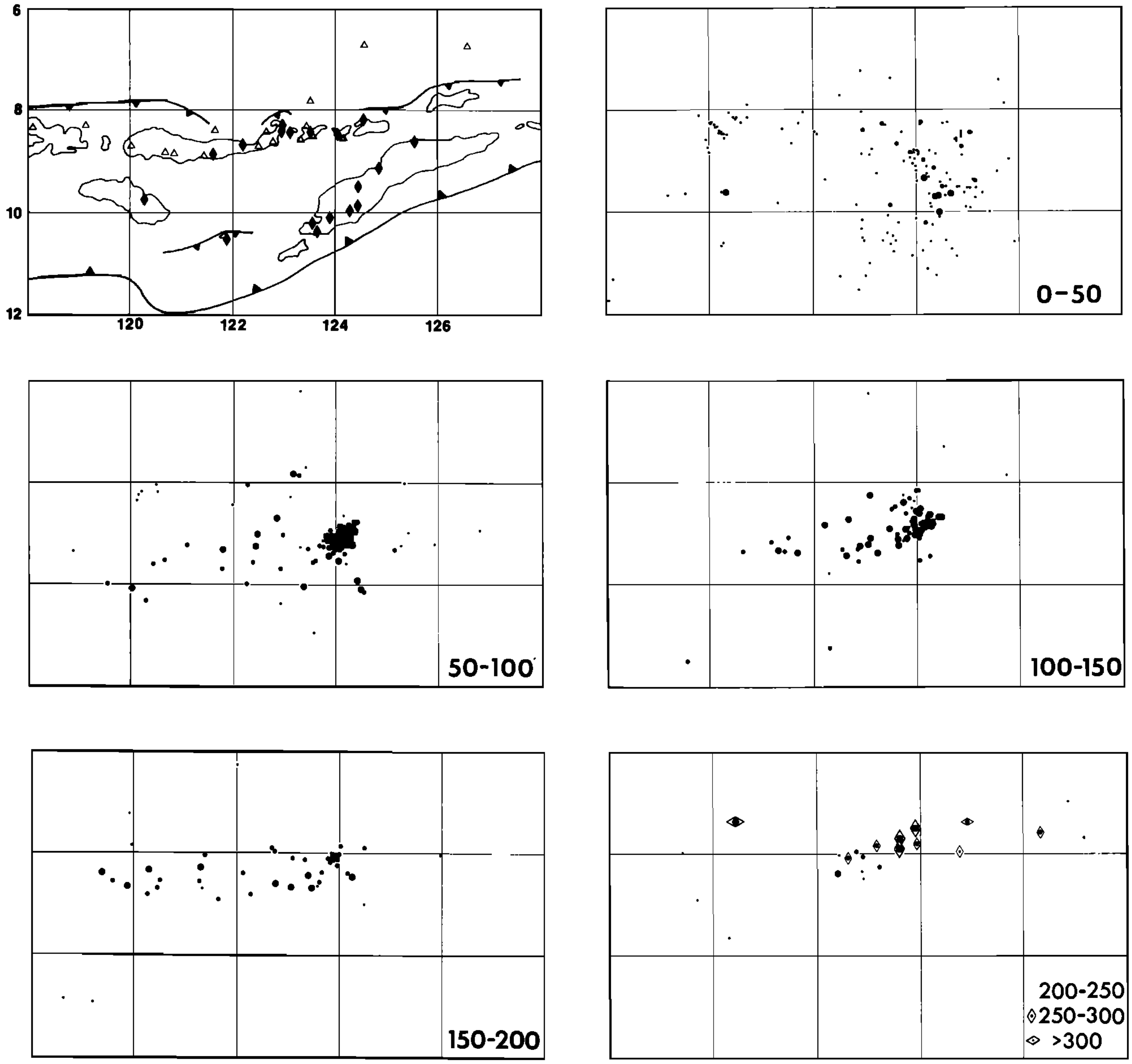

Fig. 6. Maps of earthquakes in 50-km-depth intervals (given in lower right corner of each map). Different sized symbols represent different location quality classifications starting with class A as the largest. In the upper left box, diamonds show locations of seismograph stations, and triangles represent active volcanoes.

15 and 16 north of Flores Island indicate strike slip at shallow depth along the arc.

Implications for the Development of the Collision Zone

Geologic observations on Timor support a middle Pliocene start for the collision between Australia and the Sunda arc and indicate uplift and deformation of Timor throughout the Pleistocene. The highly deformed Kolbano unit in southern Timor, consisting of bathyal radiolarites, calcilutites, and cherts of Cretaceous to Pliocene age, overlies undeformed continental shelf sediments [Barber, 1979]. The Pliocene Viqueque turbidites were deposited on top of a downfaulted block of the Kolbano unit, suggesting a middle Pliocene age for the deformation and emplacement of the Kolbano thrust sheet [Carter et al., 1976]. If the Kolbano sediments were originally from the Australian margin, as seems to be the consensus, then the above relations indicate a middle Pliocene collision with the Australian shelf. The widespread presence of the calcilutite rich, late Miocene to late Pliocene Batu Putih limestone beneath the Viqueque turbidites suggests a deep-water environment for Timor until early Pliocene time and shallowing in middle Pliocene. The Batu Putih limestone is terminated by a late Pliocene to late Pleistocene unconformity and contemporaneous folding in the south [Carter et al., 1976]. It is overlain by both a molasse facies that was folded and eroded in the early Pleistocene and middle to late Pleistocene flat-lying reefs now elevated above sealevel [Audley-Charles et al., 1974]. Since its

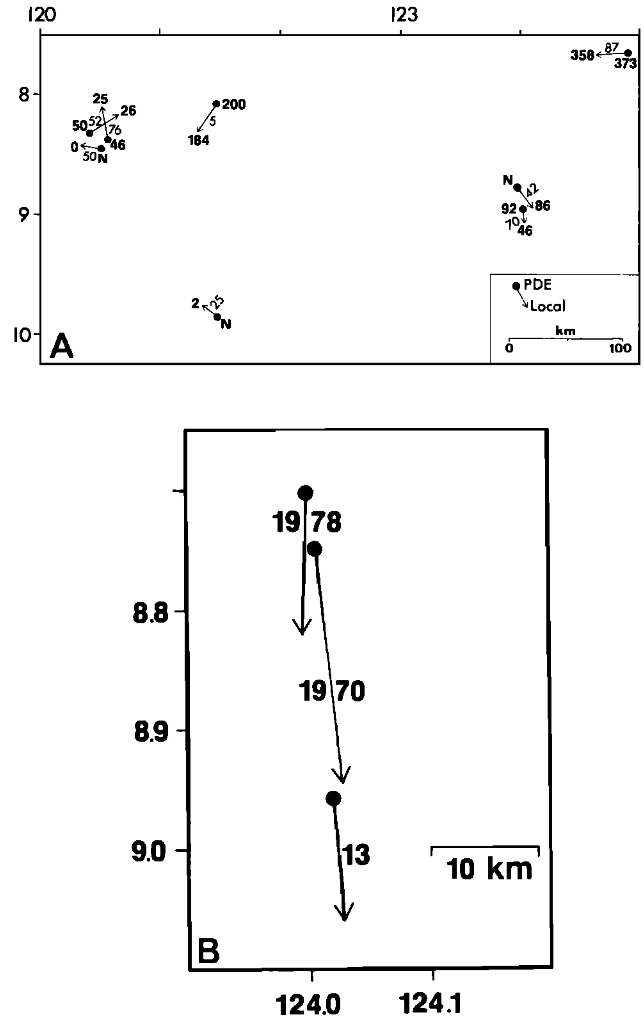

Fig. 7. (a) Comparison of locations of earthquakes determined by the local array data with those of PDE. Arrows point from the PDE location to that obtained with local data, and the numbers at either end represent the computed depths (N represents 33 km depth). Numbers along the vectors are the numbers of seismograph stations used in the PDE location. (b) Epicentral shifts relative to International Seismological Centre locations (solid circles) for the 1970 and 1978 events when relocated relative to event 13. The shift between the PDE location and that of the local network is shown for event 13.

emergence in late Pliocene time, parts of Timor have undergone 3 km of uplift. The rate of uplift for Timor and the island of Atauro is continuing at about 0.5 km/m.y. [Chappell and Veeh, 1978].

Earthquakes recorded during the temporary survey period reveal an east-northeast striking seismic zone north of Timor that dips to the northwest at about 45°. These earthquakes occur north and east of where the Australian continental slope now intersects the Timor trough (Figure 1). The strike of the seismic zone north of western Timor from 50 to 150 km depth parallels the present structural trends of both Timor and the Timor trough (Figures 3 and 6). As it is unlikely that the slab would change strike after being subducted, Timor and the trough almost certainly have been at their present trends since the time the slab presently at 150 km depth entered the trench. The distance along the seismic zone from the Timor trough to 150 km depth is approximately 300 km and hence represents about 4 m.y. of subduction at a rate of 75 km/m.y. By this calculation, subduction of the material presently at 150 km depth commenced in the mid-Pliocene, or at about the time Australia collided with the arc and Timor emerged.

The seismic zone from 300 to 500 km depth north of Timor strikes east-west and continues beneath the Sunda arc to the west and the Banda arc to the east [Cardwell and Isacks, 1978]. The continuity of strike at depth suggests that the contortion in the slab in the 70-150 km depth range north of western Timor does not extend much deeper than 150 km and is therefore a consequence of tectonic processes over the past 6 m.y. or so. The timing of initial collision of the arc with Australia, the length of the contorted portion of the seismic zone, and the average convergence rates suggest a causal relationship between the bending of the convergent margin and the arrival of Australia. Thus we infer that the introduction of continental crust into the subduction zone was responsible for the bend in the trench, in Timor, and ultimately in the slab. The outstanding implication of this inference is that the earthquakes at 150 km depth would occur within or near subducted Australian continental lithosphere.

Preliminary results of an inversion for seismic velocities using the microearthquake data presented here support the case for the presence of continental crust as deep as 150 km north of Timor (S. Roecker and R. McCaffrey, unpublished results, 1984). In the one-dimensional case, P velocities are found to be typical of the crust and upper mantle in the 0-55 km depth range. From 55 to 110 km depth, however, horizontally averaged P velocities appear to be about 10% lower than average mantle P wave velocities and about 4% lower below 150 km depth, where resolution is lost. A preliminary solution for the three-dimensional structure also shows a sharp decrease in velocity going from beneath the central Savu Sea toward Pantar and western Timor.

We suggest the following scenario for the development of the collision zone. The east-west continuity of the deeper (>300 km) seismic zone north of Timor implies that in late Miocene time the subducting trench was oriented east-west. At that time, oceanic lithosphere was being subducted beneath a forearc containing at most only a small continental fragment, of which a modern analogue may be Sumba. In Pliocene time, the northeast trending Australian continental slope intersected the trench and the buoyancy of the continental crust caused indentation of the trench axis and the arc as it forced its way northward. The thicker and less dense continental lithosphere topped by a voluminous sedimentary pile produced shallowing of the trench floor and uplift of the forearc, thus causing Timor's emergence. The uplift of the forearc probably was associated with an increased compressional stress across the entire arc structure, which inhibited further volcanism. Shortening within the forearc itself by thrust faulting (as is now observed near Savu) in the early stages of collision could account for part of the counterclockwise rotation

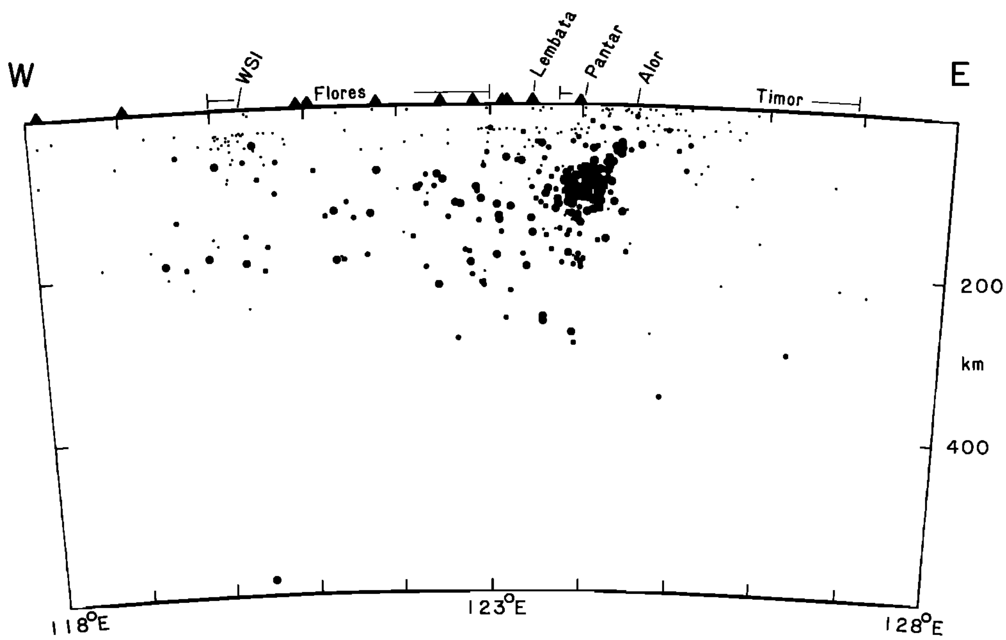

Fig. 8. Projection of all earthquakes located by the local network onto an E-W trending vertical plane (parallel to the arc). Large dots show the most reliable (A) locations, and smallest dots represent the most uncertain (C). Triangles at the surface show positions of active volcanoes. The depth of the earthquake at 580 km was taken from the PDE location [U.S. Geological Survey, 1982].

of both Timor and the Timor trough relative to the Java Trench. (The forearc near Timor is narrower than to the west where volcanism is still active.) Convergence may now be shifting to the back arc along the south directed Wetar Thrust [Hamilton, 1979; Usna et al., 1979; Silver et al., 1983].

If Australia first intersected the trench at 3-4 Ma and if subduction has slowed since 0.5 Ma [Johnston and Bowin, 1981], then approximately

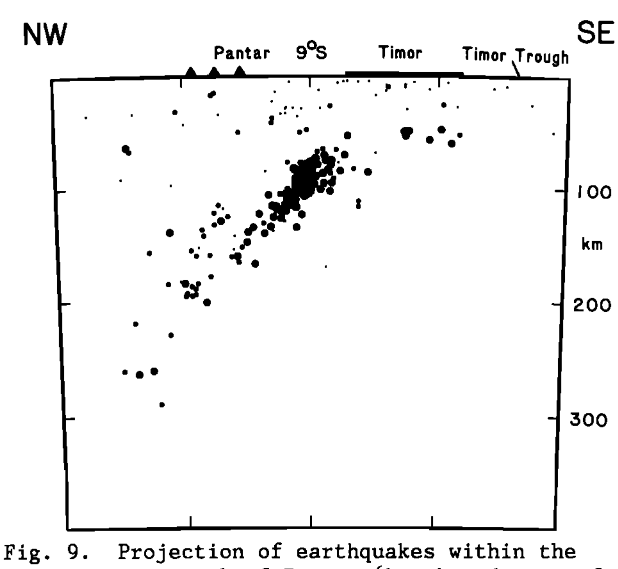

Fig. 9. Projection of earthquakes within the seismic zone south of Pantar (bracketed area of Figure 3) onto a vertical plane striking N25°W. The projection area is 120 km wide. Symbols used are as in Figure 8. The uncertainties in the locations of class A and B events (two larger symbols) are approximately 10 km or less.

250 km (at 75 km/m.y.) of the Australian margin would have been thrust beneath the Timor trough. Both gravity data [Chamalaun et al., 1976] and the exposure of continental shelf sediments from Australia extending to the north coast of Timor [Barber, 1979] suggest that continental crust underlies the island as far as its north coast (or about 125 km from the Timor trough). Thus at least half of the estimated 250 km of subducted continental crust could presently form the crust of Timor. To account for all convergence by crustal thickening beneath Timor requires that the present crustal thickness of Timor be twice that of the Australian shelf entering the trench or at least 60 km. However, gravity values over Timor do not indicate such considerable crustal thickening with material of the density of continental crust. Thus either the continental crust has in part been subducted or is imbricated with higher density oceanic crustal or mantle rocks beneath Timor. The latter explanation seems unlikely in view of the minor importance of ophiolite exposed on Timor. We suggest instead that a large portion of the subducted Australian crust is represented by the seismic zone north of west Timor from 70 to 150 km depth.

In this scenario we suggest the subduction of at least part of the continental crust to a depth of about 150 km. Roecker [1982] inferred that continental crust was subducted to 150 km beneath the Hindu Kush from his observation of low P and S wave velocities within the seismic zone. We note that in an analogous tectonic setting beneath the Hindu Kush, where the Indian continent protrudes into Asia, there are similarly a counterclockwise bend in the eastern end of the intermediate depth seismic zone, an abrupt termination of seismicity (but at both ends), and a near absence of earthquakes shallower than 70 km

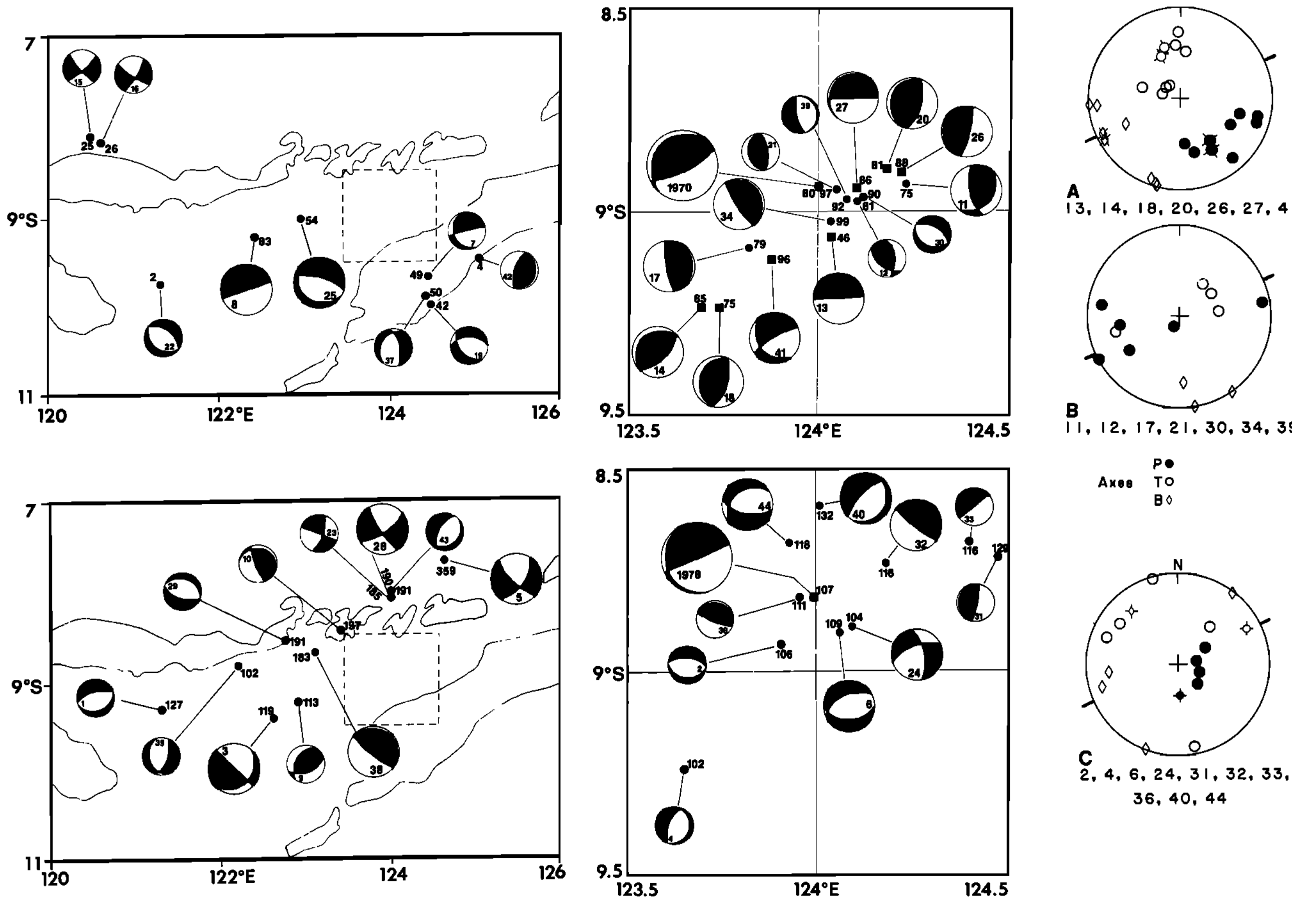

Fig. 10. Maps showing locations of fault plane solutions and their lower hemisphere representations. Numbers within the solutions are the event numbers in Table 3, and those next to the epicenter symbol are depths in kilometers. The top map shows solutions for events shallower than 100 km, and the bottom boxes show those deeper than 100 km; the right sides are for the regions south of Pantar. Shaded quadrants represent compressional first motions. The better quality solutions for the microearthquakes are represented with intermediate-sized focal spheres. Lower hemisphere projections of the well-constrained P, T, and B axes are shown on the right for the events south of Pantar. The lines on the perimeter of the projections of the axes show the trend of the seismic zone. Those earthquakes whose axes are in the upper plot (A) are shown by squares at their epicentral positions. The axes for the 1970 and 1978 events are superimposed on crosses in the plots (with group A) and those from the composite solution (45) for the upper seismic zone are superimposed on pluses (in group C).

depth, the approximate crustal thickness [Chatelain et al., 1980]. Whether or not these similar observations are characteristic of subduction of continental crust is not clear.

The material subducted to 150 km depth beneath the eastern Savu Sea may have been similar to the present-day Scott or Exmouth plateaus that are rifted continental crust and extend hundreds of kilometers out from the western Australian margin. The Scott Plateau is under 1-3 km of water yet is associated with positive free air gravity anomalies [Stagg, 1978], indicating thinner and presumably more readily subductable crust than is beneath the Australian shelf. One such plateau may have led the way into the subduction zone.

The region west of Timor, where the Scott Plateau is presently entering the Java trench, represents an earlier stage in the evolution of the collision zone. There the forearc is beginning to close up by internal thrust faulting along the Savu Thrust [Hamilton, 1979; Silver et al., 1983], and the arc is being deformed by shallow strike-slip faulting and back arc thrust faulting [McCaffrey and Nabelek, 1984b]. However, some of the deformation in this region may be due to subduction beneath a thick forearc (Sumba) rather than continental collision [Silver et al., 1983; McCaffrey and Nabelek, 1984b].

The intermediate depth seismic zone south of Pantar terminates updip beneath the north coast of Timor (Figure 9) and several fault plane solutions (i.e., group A) for earthquakes near the termination show T axes that are aligned with the dip of the slab (Figure 10). These events form a very narrow zone in map view (Figure 10, top right), suggesting that they occur along a steep rather than gently dipping fault zone. In this case, fault plane solutions indicate a north-side-down sense of relative movement for

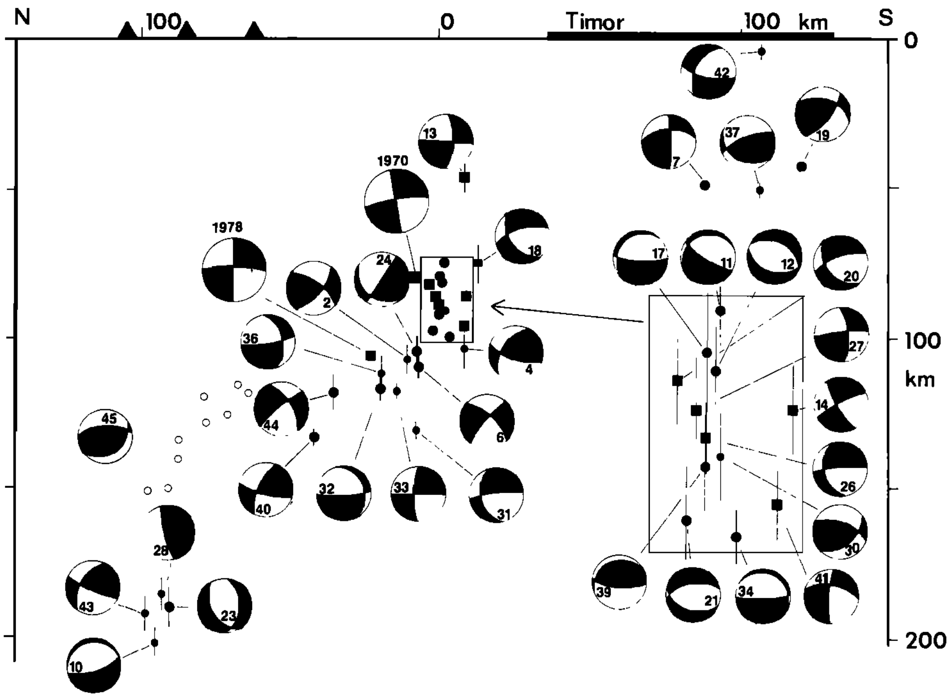

Fig. 11. Projection of fault plane solutions from the region north of western Timor onto a vertical plane striking N25°W, the same projection as in Figure 9. Solutions are presented on back hemisphere projections. Vertical bars on the hypocentral symbols are the standard deviations in depth (ERZ). Squares show the events that we suspect are related to detachment (group A of Figure 10). Open circles show the positions of the events used in the composite solution 45.

the fault zone. We note also that the 1970 and 1978 earthquakes and the two largest events recorded in this area during the survey (event 13, PDE m_b=5.4; event 27, PDE m_b=5.5) all display this type of faulting. We interpret these solutions as indicating that the slab is broken (detaching) along a steeply dipping fault (or fault system) that trends parallel to the northwest coast of Timor.

The orientations of the P and T axes in the B group of solutions may be due to the 25° bend in the slab about an axis oriented downdip. A much

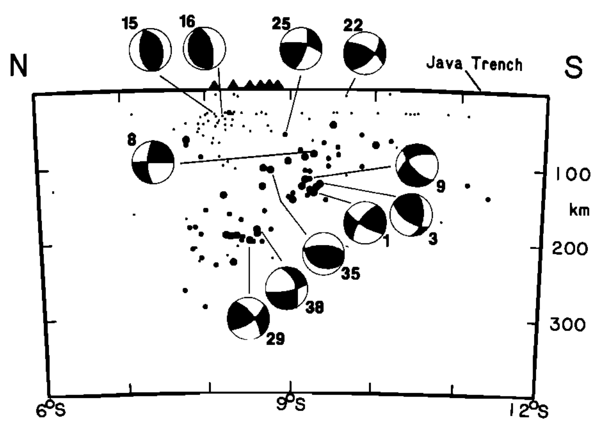

Fig. 12. Projection of all earthquakes west of 123°E onto a northerly striking vertical plane. Symbols used are as in Figure 8. Fault plane solutions are shown on back hemisphere projections.

larger bend and similar orientations of fault plane solutions are observed by Fitch and Molnar [1970] and Cardwell and Isacks [1978] at the eastern end of the Banda Arc between 127° and 130°E (Figure 2). There the plate and trench undergo a 90° bend, and P axes for intermediate depth earthquakes are, in general, parallel to the local strike of the slab (Figure 2), suggesting that the bending produces compression in the slab. No extensional type events have been found on the convex side of the slab, as would be expected from the hypothesis that the stresses are generated by bending.

In the seismic zone north of Timor, however, both compressional (solutions 11, 12, 17, 21, and 34) and extensional (30 and 39) fault plane solutions are found (Figure 10). For a concave northwest bend in a northwest dipping plate, the reverse faulting solutions would be expected in the top (or northwestern) side of the plate, while the normal faulting events would be expected deeper and to the southeast. Unfortunately, the large uncertainties in hypocentral depths relative to the thickness of the seismic zone (Figure 11) obscures the spatial relationship between the different type mechanisms.

Although the P axes for the reverse faulting solutions north of Timor and beneath the eastern Banda arc (Figure 2) are aligned roughly parallel to the strike of the slab, the B axes are not aligned downdip as would be predicted by a model of simple flexure about an axis parallel to the dip direction of the plate. The observed variations in stress orientation within the upper part of the slab could be explained by bending, however, if the subducted plate was detached as

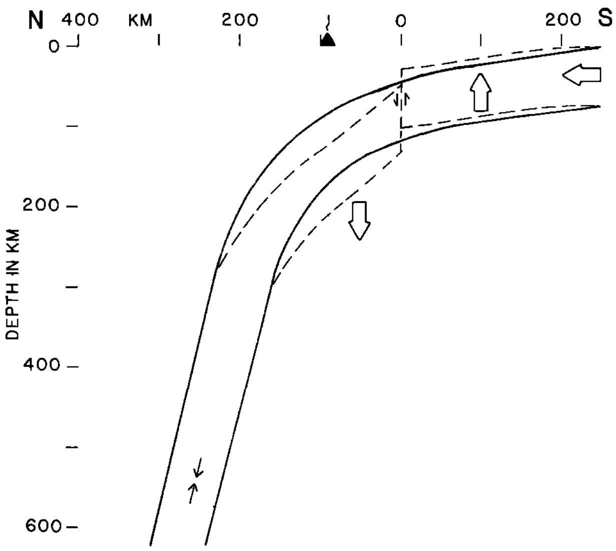

Fig. 13. A simple interpretation of detachment of the deeper subducted lithosphere north of Timor. The solid line represents the configuration prior to detachment, which probably also exists today north of the Java trench. The dashed line shows the configuration after detachment has commenced. The large arrows show the directions of motion of various parts of the slab relative to an inert, deep mantle. Small arrows show the expected orientations of principal stresses within the postdetachment slab and the senses of relative motion on surfaces. The figure is drawn to scale with the origin at approximately 9°S.

shown in Figure 13. Because the mantle's viscosity (inferred from postglacial rebound) is not high enough to support the slab with its upper end free [Davies, 1980], the upper part of the detached slab would sink more rapidly if it was detached. The lower part of the detached slab would remain under compression due to the weight of the slab above and prevent the upper part of the slab from sinking along the inclined path. Thus the upper part of the slab and hence the B axes would become more horizontal as it sinks. The sinking and increased flexure would likely produce varied directions for the P and T axes within the upper part of the slab.

Lateral Variations in Seismicity

East of about 124.5°E, microseismicity, like the distribution of larger earthquakes, is much lower than to the west. The seismic zone appears to end along a northwest trending break in the 50-200 km depth range (Figures 3 and 6) that underlies the easternmost active volcano (Pantar) of the Sunda arc (Figure 8), suggesting a relationship between the seismic and volcanic quiescence within the collision zone. Beneath the stretch from Pantar to Damar, where there are no volcanoes, Cardwell and Isacks [1978] report only two earthquakes in the 71-300 km depth range and both occur near the extremities of the quiet zone: one at about 200 km depth is near Damar and the other is at 260 km depth beneath the northern part of the zone (event 37 in Figure 2 is at 387 km depth). It is unresolvable whether the slab ends along the northwest trending break beneath Pantar or is merely aseismic. To the east where the slab undergoes a 90° bend beneath the Banda arc, however, at the same depths, seismic activity is very high [Cardwell and Isacks, 1978].

The seismic quiescence at intermediate depths north of Timor might indicate that detachment is complete and the slab is under small deviatoric stress as it sinks freely. In the region of the Banda arc east of 124°E, with the possible exceptions of earthquakes in 1963 [Osada and Abe, 1981] and 1981 [Michael-Leiba, 1984], all fault plane solutions for intermediate depth earthquakes (Figure 2) show the P axes along strike of the slab, characteristic of flexure about an axis parallel to the dip of the slab. There are none that show the stress orientations usually observed in subducted slabs (downdip P or T axes and B axes parallel to strike [Isacks and Molnar, 1971]). This suggests that bending is the major cause of stresses that produce earthquakes in the slab beneath the Sunda and Banda arcs. It follows that the quiescence at intermediate depths north of central Timor is perhaps due to the lack of a bend and therefore of sufficient stress to cause earthquakes in that area. The abrupt truncation of the seismic zone north of western Timor (that probably represents a bend in the slab) may indicate a tear that acts to decouple it from the seismically quiet portion north of central Timor.

Summary

The locations of approximately 450 microearthquakes recorded by a local seismograph network are presented and used to examine the configuration of the seismic zone along the Australia-Sunda arc convergent margin near Timor Island. Although the network operated for only 10 weeks, many features of the observed seismicity patterns are also noticeable in the distribution of larger earthquakes [Hamilton, 1974; Cardwell and Isacks, 1978].

Near Pantar Island, a seismic zone between 70 and 200 km depth suggests that the north dipping slab strikes N65°E, parallel to Timor and to the Timor trough rather than to the overall trend of the convergent margin which strikes east-west. This represents a 25° counterclockwise bend in the subducted plate. We assume that the contortion was produced at the time the slab was at the surface of the earth and not after it had been subducted. The length of the seismic zone and the rate of convergence imply that the present-day 150-km slab contour was subducted at about 4 Ma or about the time Australia collided with the Sunda arc and Timor was elevated above sea level. We infer, then, that the presence of buoyant Australian continental crust in the subduction zone produced the bend in the surface features and the contortion in the slab; this implies that the bent portion of the subducted slab was once part of the thick crust of the Australian margin.

Fault plane solutions show considerable variation in orientations, but some patterns are observable. Several fault plane solutions from the southern and shallower portion of the seismic zone north of Timor reveal steep nodal planes that strike parallel to the seismic zone and

indicate a north-side-down sense of relative motion. These fault plane solutions are interpreted to be due to a detachment fault within the subducted slab. In the same region many fault plane solutions show P and T axes that vary in plunge but lie in a near vertical plane that parallels the strike of the seismic zone. We interpret these as due to bending stresses within the top of the slab as it sinks. Finally, the tendency for regions of high levels of intermediate depth earthquake activity to be associated with cross slab compressional stresses suggests that bending about inclined axes is responsible for most of the earthquakes within the slab. This mechanism may explain the great lateral variation in seismicity at intermediate depths beneath the Sunda and Banda arcs.

Appendix

Field Procedures

For 10 weeks between June and September of 1982 we operated 15 portable seismographs on the islands surrounding the Savu Sea (Figure 1 and Table 1). In addition, we obtained records from the permanent short-period seismograph stations (MKS, WSI, and KUG) that are part of the southeast Asian regional network [Hodgson, 1980]. All temporary stations recorded on smoked paper and used 1-Hz vertical seismometers, while one horizontal component was used at Adonara for a short time. Recording speeds were 60 mm/min except those at Ende, Maumere, Pantar, and Kefamenanu, which were 120 mm/min. The permanent stations have 1-Hz vertical seismometers and record at 60 mm/min using paper and ink.

Time synchronization was obtained in the field by recording the broadcasted WWV time signal on the seismograms. Clock drift for most instruments was linear over long periods of time and was assumed to be likewise between checks. There were no large jumps in the time corrections, indicating that the drift is more likely due to maladjustment of the oscillator than to discrete glitches. Uncertainties associated with clock corrections for each station were estimated from the scatter of the individual measurements about straight-line segments through the points and are given as σ in Table 1. The actual errors in the clock corrections are smaller than those cited because the corrections used were biased toward the clearer time signals. (Frequently, a second time signal of unknown origin was received that differed from WWV by 0.5 s but was easily distinguished from the WWV signal.)

Data Analysis

Using a digitizing table, we measured arrival times with a resolution of 0.025 s for recording speeds of 60 mm/min. To estimate the possible error caused by the variation in drum speeds, we measured arrival times relative to instrument time marks both before and after the arrivals; such arrival times consistently differed by 0.05 s or less. The largest error in measuring the arrival times is due to the uncertainty in identifying the onsets of the phases, but because the majority of picks were made by one person (R. McCaffrey), we expect this error to be largely systematic. Systematic errors result in a shift in the origin time of the earthquake but not in the hypocenter. Because most of the arrivals from the local earthquakes were impulsive, the random part of the error in arrival times is probably less than 0.10 s.

Earthquakes were located with the computer program HYPOINVERSE [Klein, 1978] using a layered, flat earth P wave velocity model and a constant P to S wave velocity ratio. The validity of using flat earth models for arrays of this size was demonstrated by Chatelain et al. [1980]. In determining the locations and takeoff angles presented here, we used P wave velocities similar to the average earth values of Herrin [1968] (Table 2) and a V_p/V_s ratio of 1.75 (discussed below). The classifications A, B, and C (in order of decreasing reliability) were made according to the root-mean-square (rms) error in the travel time residuals, standard deviations in the epicenter (ERH) and in the depth (ERZ), the distribution and number of stations recording the event, and the number of P and S phases used to constrain the location. The criteria for and the uncertainties associated with each classification were determined by examining the variations in the calculated locations of several events due to perturbations in the assumed velocity model, V_p/V_s ratio, and group of stations and phases used in locating the event. The results of these tests will be discussed first.

Subsets of the recording array. Because smaller events are normally recorded by a subset of the stations, relative mislocations can arise from differences in the number and distribution of recording stations. In order to examine the effects of a changing station geometry, we relocated many of the better recorded events several times while changing the number of stations and phases used in the location. For events south of Pantar, calculated locations are stable (i.e. within 10 km of one another in both epicentral position and depth) when five or more phases are used. Surprisingly, the omission of S phases does not significantly alter the locations of the events in that area. Stability for events southeast of Timor is obtained by having at least seven phases among which the presence of at least one S phase is crucial. For events beneath the Savu Sea, five phases give a stable epicentral location, but an S phase gives important information on the depth. Epicenters north of Flores are stable with six phases if one is an S phase, but depths of shallow events there can be in error by 50 km or so. Hypocentral locations southwest of Sumba are unstable with up to 10 phases even with S phases included. In general, stable locations are assured throughout the area by at least seven phases including one or more S phase, and we require that our most reliable locations (classification A) meet this criterion. For the most active region south of Pantar, fewer phases are needed, and an S phase is not critical.

V_p/V_s Ratio. For events with S wave arrivals, the calculated depth is sensitive to the choice of the V_p/V_s ratio. For example, we relocated ten events using V_p/V_s ratios ranging from 1.70 to 1.80 and found that the depths became shallower by 10-50 km without significantly different rms residuals. To estimate V_p/V_s

from the arrival time data, Wadati plots were made for 20 events having more than eight clear S arrivals. A best fitting line was determined for the data from each earthquake and the average slope gave a value of 1.75 for V_p/V_s with a standard deviation of 0.03, which maps to an absolute uncertainty in depth of 3-15 km. The error in depth due to an erroneous V_p/V_s ratio is systematic, however, so the relative errors in depth will be less than this.

Crustal structure. Thirty representative events were relocated using a variety of assumed thicknesses and seismic velocities for a crustal layer over a mantle halfspace (V_p=8.1 km/s). First, the crustal velocity was held at 6.5 km/s, while the Moho was placed at 20, 30, and 40 km depth. Second, crustal thickness was fixed at 30 km, while the crustal P wave velocities of 6.0, 6.5, 7.0, and 7.5 km/s were used. These general combinations cover the spectrum of probable structures for the upper 150 km of the earth beneath the survey area and include models both faster and slower than the velocity model used in the locations (Table 2). For the range of structures, the average differences (with respect to the solution using the model in Table 2) in calculated depths and epicenters for events subsequently classified as A were 6 and 2 km, respectively. For B events, they were 13 and 8 km. Events subsequently classified as C had average differences similar to those for the B events but with a larger standard deviation.

We defined quality A locations to be those based on a minimum of seven phases including one S unless there are more than 10 P arrivals, with an rms residual of less than 1.0 s but greater than 0.1 s, recorded by stations in at least three quadrants, with at least one station at a distance less than the focal depth, and whose covariance matrix from HYPOINVERSE has horizontal (ERH) and vertical (ERZ) projections of the principal axes less than 10 km in length. The locations of events that meet these requirements probably have relative uncertainties of 5 km in both depth and epicentral coordinates in the region south of Pantar and of twice these values at the edges of the array. Absolute uncertainties due to systematic mislocations are likely larger than this. Events classified as B are those non-A events that were located with five or more phases (not necessarily including an S), with rms less than 2.0 s, recorded by stations in at least two quadrants, with an ERH of less than 10 km and ERZ of less than 30 km, and with one station at a distance less than twice the focal depth. The uncertainties in the locations of B events in general are twice those of A events for a given location. C events are those remaining, with more than four phases and with an rms of less than 3.0 s. The uncertainties in locations of C events can vary greatly depending on which criterion the event fails but probably are similar to those of B events when inside the array. The calculated depths of C events probably are not reliable.

Fault Plane Solutions

Takeoff angles were determined using the P wave velocities in Table 2. The uncertainties in takeoff angles for upgoing rays due to uncertainties in the structure and focal depths are only a few degrees, but for downgoing rays the errors can be tens of degrees. The rays from the intermediate depth earthquakes to the local stations are for the most part upgoing and therefore reliably estimated. An inherent degree of uncertainty must be added to the fault plane solutions of the shallowest events. Although most of the rays were upgoing, the first motion data are presented on lower hemisphere plots for clarity.

First motions were classified as being either "strong" or "weak" and are presented as large and small symbols in Figure 4. "Weak" is not meant to imply uncertainty in polarity but rather a small amplitude that could be due to either a near nodal ray, high attenuation, or low instrument magnification. In fitting the nodal planes to the observed data, we attempted to keep "strong" arrivals toward the center of quadrants while satisfying all polarity readings. For several events, two quite different solutions were obtained from the first motion data, in which case the alternative solution is shown by dashed lines in Figure 4. An attempt was made to grade the solutions based on the reliability with which the nodal planes were determined. The criteria for a good solution are that all possible solutions show the same type of faulting and that the strikes of the steeper planes do not vary by more than 30° or so.

Although one of the nodal planes for the fault plane solution may be poorly constrained, there may be some useful information about the orientation of the P or T axes in the first motion data. In order to assess the consistency of the inferred orientations of the principal stresses, we examined each of the P, T, and B axes to determine whether or not they are constrained by the first motion data. For example, solution 21 (Figure 4) has poorly constrained nodal planes and T and B axes, but the P axis does not change significantly in the alternative solution. In the plots of P, T, and B axes in Figure 10, only the well-constrained axes are used.

Waveform Data

For the earthquakes of 1970 and 1978, long-period P and SH waveforms were used to determine the depths and fault plane solutions by a formal inversion procedure. The waveforms were digitized at 0.5-s intervals and a least squares fit was made to a double-couple, point source model that was parameterized by strike, dip, slip, centroidal depth, and a variable number of triangular time function elements from which the scalar seismic moment and duration of faulting were derived. Because the depth estimate is dependent on the assumed velocity structure, we used a source velocity structure similar to that used to locate the microearthquakes (Table 2) so depths could be compared directly (i.e., systematic errors will be similar for both groups). The errors in depths for the 1970 and 1978 earthquakes relative to the assumed velocity structure are quite small (approximately 5 km). The methods are described in more detail by Nabelek [1984].

The fault plane solutions determined for the two earthquakes are similar to each other and to several of those from microearthquakes in that they show a steep nodal plane that strikes roughly parallel to the strike of the seismic zone south of Pantar. The depths are also similar to those of the microearthquakes. We relocated the epicenters of the 1970 and 1978 events relative to event 13, the largest event recorded from the region south of Pantar during the microearthquake survey in 1982, using Herrin P wave travel time tables. The epicenters of the earlier earthquakes were recalculated using P arrival times at only those stations recording event 13 and with individual station corrections equal to the travel time residual at the station for event 13. The resulting shifts in the epicenters are similar to those observed between the PDE locations of the 1982 events and the locally determined epicenters (Figure 7), about 15 km to the south.

Acknowledgments. Arrangements for the field work in Indonesia were made with the generous support of H. M. S. Hartono of the Geological Research and Development Centre (PPPG), J. Widartoyo of the Ministry of Mines, and C. Sutrisno of the Institute of Meteorology and Geophysics (BMG). M. Untung and I. Usna of PPPG and R. Soetardjo of BMG supplied instruments and arranged for field assistants. We were aided in the field by J. L. Chatelain (Office de la Recherche Scientifique et Technique Outre-Mer, Noumea); K. Hardjawidjaksana, E. Kertapati, T. Kuntoro, J. Nasution, and A. Sukarna (PPPG); S. Anie, J. Kartusuwita, S. Patmowidodo, P. Y. Prih Haryadi, and M. Riyadi (BMG); H. Lyon-Caen (Massachusetts Institute of Technology); and D. Reed (Scripps Institute of Oceanography). We thank P. Donoho, C. Frohlich, and B. M. Larue for their assistance. Generous support in the field was given by many people associated with the Meteorological stations throughout the study region. Comments on versions of the manuscript were made by M. G. Audley-Charles, R. K. Cardwell, J. W. Dewey, H. Lyon-Caen and W. Spence. This work was supported by National Science Foundation grants EAR-8115909 and EAR-8319250.

References

Audley-Charles, M. G., D. J. Carter, and A. J. Barber, Stratigraphic basis for tectonic interpretations of the outer Banda arc, eastern Indonesia, Proc. Annu. Conv. Indones. Petrol. Assoc. 3, 25-44, 1974.

Barber, A. J., Structural interpretations of the island of Timor, eastern Indonesia, Proc. Southeast Asian Petrol. Explor. Soc. 4, 9-21, 1979.

Beck, R. H., and P. Lehner, Oceans, new frontier in exploration, Am. Assoc. Pet. Geol. Bull., 58, 376-395, 1974.

Bowin, C. O., G. M. Purdy, C. Johnston, G. G. Shor, L. Lawver, H. M. S. Hartono, and P. Jezek, Arc-continent collision in the Banda Sea region, Am. Assoc. Pet. Geol. Bull., 64, 868-915, 1980.

Cardwell, R. K., and B. L. Isacks, Geometry of the subducted lithosphere beneath the Banda Sea in eastern Indonesia from seismicity and fault plane solutions, J. Geophys. Res., 83, 2825-2838, 1978.

Carter, D. J., M. G. Audley-Charles, and A. J. Barber, Stratigraphical analysis of island arc-continental margin collision in eastern Indonesia, J. Geol. Soc. London, 132, 179-198, 1976.

Chamalaun, F. H., Palaeomagnetic evidence for the relative positions of Timor and Australia in the Permian, Earth Planet. Sci. Lett., 34, 107-112, 1977a.

Chamalaun, F. H., Palaeomagnetic reconnaissance result from the Maubisse formation and its tectonic implications, Tectonophysics, 32, 17-26, 1977b.

Chamalaun, F. H., K. Lockwood, and A. White, The Bouguer gravity field of eastern Timor, Tectonophysics, 30, 241-259, 1976.

Chamalaun, F. H., A. E. Grady, C. C. von der Borch, and H. M. S. Hartono, Banda Arc tectonics: The significance of the Sumba Island (Indonesia), Mem. Am. Assoc. Pet. Geol., 34, 361-375, 1982.

Chappell, J., and H. H. Veeh, Late Quaternary tectonic movements and sea-level changes at Timor and Atauro Island, Geol. Soc. Am. Bull., 89, 1189-1198, 1978.

Chatelain, J. L., S. W. Roecker, D. Hatzfeld, and P. Molnar, Microearthquake seismicity and fault plane solutions in the Hindu Kush region and their tectonic implications, J. Geophys. Res., 85, 1365-1387, 1980.

Curray, J. R., G. G. Shor, R. W. Raitt, and M. Henry, Seismic refraction and reflection studies of crustal structure of the eastern Sunda and western Banda arcs, J. Geophys. Res., 82, 2479-2489, 1977.

Davies, G. F., Mechanics of subducted lithosphere, J. Geophys. Res., 85, 6304-6318, 1980.

Engdahl, E. R., and C. H. Scholz, A double Benioff zone beneath the central Aleutians: An unbending of the lithosphere, Geophys. Res. Lett., 4, 473-476, 1977.

Fitch, T. J., Earthquake mechanisms and island arc tectonics in the Indonesian-Philippine region, Bull. Seismol. Soc. Am., 60, 565-591, 1970.

Fitch, T. J., Plate convergence, transcurrent faults and internal deformation adjacent to southeast Asia and the western Pacific, J. Geophys. Res., 77, 4432-4460, 1972.

Fitch, T. J., and W. Hamilton, Reply, J. Geophys. Res., 79, 4982-4985, 1974.

Fitch, T. J., and P. Molnar, Focal mechanisms along inclined earthquake zones in the Indonesian-Philippine region, J. Geophys. Res., 75, 1431-1444, 1970.

Given, J. W., and H. Kanamori, The depth extent of the 1977 Sumbawa, Indonesia earthquake (abstract), Eos Trans. AGU, 61, 1044, 1980.

Grady, A. E., A reinvestigation of thrusting in Portguese Timor, J. Geol. Soc. Aust., 22, 223-228, 1975.

Hamilton, W., Earthquake map of the Indonesian region, U.S. Geol. Surv. Misc. Invest. Ser. Map, I-875-C, 1974.

Hamilton, W., Subduction in the Indonesian region, in Island Arcs, Deep Sea Trenches, and Back-Arc Basins, Maurice Ewing Ser. vol. 1, edited by M. Talwani and W. C. Pitman III, pp. 15-31, AGU, Washington, D. C., 1977.

Hamilton, W., Tectonics of the Indonesian region, U.S. Geol. Surv. Prof. Pap., 1078, 345 pp., 1979.

Hasegawa, A., N. Umino, and A. Takagi, Double-planed structure of the deep seismic zone in the northeastern Japan arc, Tectonophysics, 47, 43-58, 1978.
Hatherton, T., and W. R. Dickinson, The relationship between andesitic volcanism and seismicity in Indonesia, the Lesser Antilles, and other island arcs, J. Geophys. Res., 74, 5301-5310, 1969.
Herrin, E., 1968 seismological tables for P phases, Bull. Seismol. Soc. Am., 58, 1193-1352, 1968.
Hodgson, J. H., A short-period seismograph network in southeast Asia, Bull. Seis. Soc. Am., 70, 385-392, 1980.
Isacks, B., and P. Molnar, Distribution of stresses in the descending lithosphere from a global survey of focal mechanism solutions of mantle earthquakes, Rev. Geophys. Space Phys., 9, 103-174, 1971.
Jacobson, R. S., G. G. Shor, R. M. Kieckhefer, and G. M. Purdy, Seismic refraction and reflection studies in the Timor-Aru trough system and Australian continental shelf, Mem. Am. Assoc. Pet. Geol., 29, 209-222, 1979.
Johnston, C. R., and C. O. Bowin, Crustal reactions resulting from the mid-Pliocene to Recent continent-island arc collision in the Timor region, BMR J. Aust. Geol. Geophys., 6, 223-243, 1981.
Kappel, E. S., Plate convergence in the Sunda and Banda arcs, B.A. thesis, 40 pp., Cornell Univ., Ithaca, N.Y., 1980.
Klein, F. W., Hypocenter location program HYPOINVERSE, U.S. Geol. Surv. Open file Rep. 78-694, 1978.
McCaffrey, R., Evidence for lateral segmentation of the subducted Australian-Indian plate beneath the Banda arc near western Timor (abstract), Eos Trans. AGU, 62, 949, 1981.
McCaffrey, R., and J. Nabelek, The geometry of backarc thrusting along the eastern Sunda arc, Indonesia: Constraints from earthquake and gravity data, J. Geophys. Res., 89, 6171-6179, 1984a.
McCaffrey, R., and J. Nabelek, Depths and source mechanisms of earthquakes from the eastern Sunda arc, Indonesia (abstract), Eos Trans. AGU, 65, 997, 1984b.
McCaffrey, R., et al., Preliminary results of the 1982 microearthquake survey in Nusa Tenggara Timur, Indonesia, Bull. Geol. Res. Dev. Cent. Bandung Indones., 10, 1-9, 1984.
McKenzie, D. P., Speculations on the consequences and causes of plate motion, Geophys. J. R. Astron. Soc., 18, 1-18, 1969.
Michael-Leiba, M. O., The Banda Sea earthquake of 24 November 1983: Evidence for intermediate depth thrust faulting in the Benioff zone, Phys. Earth Planet. Inter., 36, 95-98, 1984.
Minster, J. B., and T. H. Jordan, Present-day plate motions, J. Geophys. Res., 83, 5331-5354, 1978.
Molnar, P., and D. Gray, Subduction of continental lithosphere: Some constraints and uncertainties, Geology, 7, 58-62, 1979.
Morris, J. D., Continental contamination in the Banda arc: Pb-Nd isotopic evidence for 3-component mixing (abstract), Eos Trans. AGU, 64, 906-907, 1983.
Nabelek, J., Determination of earthquake source parameters from inversion of body waves, Ph. D. thesis, Mass. Inst. of Technol., Cambridge, 1984.
Osada, M., and K. Abe, Mechanism and tectonic implications of the great Banda Sea earthquake of November 4, 1963, Phys. Earth Planet. Inter., 25, 129-139, 1981.
Roecker, S. W., Velocity structure of the Pamir-Hindu Kush region: Possible evidence of subducted crust, J. Geophys. Res., 87, 945-959, 1982.
Silver, E. A., D. R. Reed, R. McCaffrey, and Y. Joyodiwiryo, Back arc thrusting in the eastern Sunda arc, Indonesia: A consequence of arc-continent collision, J. Geophys. Res., 88, 7429-7448, 1983.
Stagg, H. M. J., The geology and evolution of the Scott Plateau, APEA J., 18, 34-43, 1978.
Usna, I., S. Tjokrosapoetro, and S. Wiryosujono, Geological interpretation of a seismic reflection profile across the Banda Sea between Wetar and Buru islands, Bull. Geol. Res. Dev. Cent. Bandung Indones., 1, 7-15, 1979.
U.S. Geological Survey, Preliminary determination of epicenters, Arlington, Va., 1982.
von der Borch, C. C., Continent-island arc collision in the Banda arc, Tectonophysics, 54, 169-193, 1979.
Whitford, D. J., W. Compston, I. A. Nicholls, and M. J. Abbott, Geochemistry of late Cenozoic lavas from eastern Indonesia: Role of subducted sediments in petrogenesis, Geology, 5, 571-575, 1977.
Whitford, D. J., and P. A. Jezek, Origin of late Cenozoic lavas from the Banda Arc, Indonesia: Trace element and Sr isotope evidence, Contrib. Mineral. Petrol., 68, 141-150, 1979.

Y. Joyodiwiryo, Marine Geological Institute of the Geological Survey of Indonesia, Jalan Dr. Junjunan 236, Bandung, Indonesia.

R. McCaffrey, P. Molnar, and S. Roecker, Department of Earth, Atmospheric, and Planetary Sciences, Massachusetts Institute of Technology, Cambridge, MA 02139.

(Received July 2, 1984;
revised November 9, 1984;
accepted November 27, 1984.)